Shallow implanted SiC spin qubits used for sensing an internal spin bath and external YIG spins.

Jérôme Tribollet, Dominique Muller, Stephane Roques, Jeremy Bartringer, Thomas Fix

Shallow implanted SiC spin qubits used for sensing an internal spin bath and external YIG spins.

Jérôme Tribollet,[*,†] Dominique Muller,[‡] Stephane Roques,[‡] Jeremy Bartringer,[‡] and Thomas Fix[‡]

Institut de Chimie de Strasbourg, Universite de Strasbourg and CNRS, UMR 7177, 4 rue Blaise Pascal, CS 90032, F-67081 Strasbourg Cedex, France, and Laboratoire Icube, Universite de Strasbourg and CNRS, UMR 7357, 23 rue du Loess, BP 20, 67037 Strasbourg Cedex 2, France

E-mail: tribollet@unistra.fr

Abstract

Silicon vacancies (VSi) color centers in bulk SiC are excellent electron spin qubits. However, most spin based quantum devices require shallow spin qubits, whose dynamics is often different from bulk one. Here, we demonstrate i/ a new method for creating shallow VSi (V2) spin qubits below the SiC surface by low energy ion implantation through a sacrificial SiO_2 layer, ii/ that those shallow VSi are dipolar coupled to an electronic spin bath, analysing Hahn echo decay, dynamical decoupling (DD), and optically pumped pulsed electron electron double resonance experiments (OP-PELDOR), iii/ that their coherence time increase with cooling the spin bath (from 55μs at 297K to 107μs at 28K), and that it can be further extended to 220μs at 100K by DD, thus demonstrating their relevance for PELDOR-based quantum sensors and processors. Finally, iv/ external spins sensing is demonstrated by the shift of the Vsi magnetic resonance lines induced by the dipolar stray magnetic field of a nearby ferrimagnetic YIG film.

[*]To whom correspondence should be addressed
[†]Institut de Chimie
[‡]Laboratoire ICube

1 Introduction

It is well known that silicon vacancies (VSi) color centers in silicon carbide (SiC), created far in the bulk by electron[1,2] or proton[3] irradiation, or during growth,[4] are highly quantum coherent electron spin qubits, even at room temperature. Recently, methodologies for single 4H-SiC silicon vacancies spin qubit ODMR (optically detected magnetic resonance) spectroscopy were demonstrated, for both single V1 silicon vacancies[5] and single V2 silicon vacancies,[6] further demonstrating the potential of those SiC spin qubits. The potential of those silicon vacancies color centers spin qubits in 4H-SiC for developping a relevant spin-photon interface was also recently underlined,[5] suggesting the possibility of a futur large scale quantum network, interfacing those spins qubits with photons travelling in optical fibers.

While many things have been demonstrated on bulk Vsi spin qubits, the study of shallow color centers spin qubits in SiC remains to be done. Beyond the fundamental interest, this study is also highly technologically relevant because many proposed spin based SiC quantum devices, like quantum sensors,[4,7] quantum processors[8] and single quantum photon source,[9] require quantum coherent shallow color centers spin qubits, located below the SiC surface, between few nm[4,7] and hundreds of nm,[8,9] depending on the targeted application, as illustrated on Fig.1. In this field of shallow spin qubits in semiconductors, it is also well known from previous studies performed for example with shallow NV- centers in diamond,[10] that various kinds of additionnal noise and thus additional decoherence exist for color centers spins located nearby the surface of the semiconductor. It is thus reasonable to assume that the same occurs in the SiC semiconductor. SiC has however the advantage over diamond of a more mature SiC semiconductor technology for nanoelectronics and nanophotonics, which could be also an advantage for quantum technologies.[7–9] While arrays of shallow VSi color centers have already been created with success by low energy ion implantation in SiC through a mask[11] or using a focused ion beam,[12] almost nothing is known about their intrinsic quantum spin coherence and more broadly about their spin dynamics, near surfaces or interfaces. Only Ramsey and Rabi experiments, performed on shallow silicon vacancies spin ensembles created by ions implantation in SiC, and using an on chip copper wire to bring microwave

to the spins, have been performed[13] to date. Very short decay times of the Ramsey and Rabi oscillation were observed,[13] in the range of hundreds of nanoseconds. However, it is well known that the Ramsey decay reflects inhomogeneous broadening, and that the Rabi oscillation damping time also contains many effects, including inhomogeneities of the applied microwave field (important in studies using microwave chip), inhomogeneities of the magnetic parameters of the spin hamiltonian (like distribution of g factor or of the zero field splitting), as well as dipolar couplings when measurements on spin ensembles are performed.[14,15] Thus, nothing about the intrinsic T2 spin coherence time, as usually obtained by Hahn spin echo decay,[2,7,18] and about T1, the spin lattice relaxation time, as usually obtained by inversion recovery,[2,7,18] can be extracted from those kind of Ramsey and Rabi measurements on spin ensembles.

With in mind the idea of developping hybrid paramagnetic-ferromagnetic SiC based quantum processors or sensors, as recently proposed,[4,7,8] here we first demonstrate a new methodology for creating shallow VSi spin qubits located at a controlled nanoscale distance below the SiC surface by low energy ion implantation through a sacrificial SiO_2 layer, and then, we demonstrate by various magnetic resonance methods, that our shallow silicon vacancies spin qubits are 1/ coupled to an electronic spin bath, 2/ can be also coupled to the stray magnetic field of a nearby YIG ferrimagnetic thin film, and 3/, that despite the interaction with the spin bath, they remain quantum coherent, even at room temperature, which is quite promising for the development of quantum sensors and processors based on shallow Vsi spin qubits in 4H-SiC.

2 Experiments and Results

Ion implantation technology is particularly well suited to create shallow silicon vacancies in SiC at a controlled nanoscale depth. This is due to the fact that controlling the ions energy allows the control of the average depth <z> of the ions positions in the solid,[16] and also the position of the

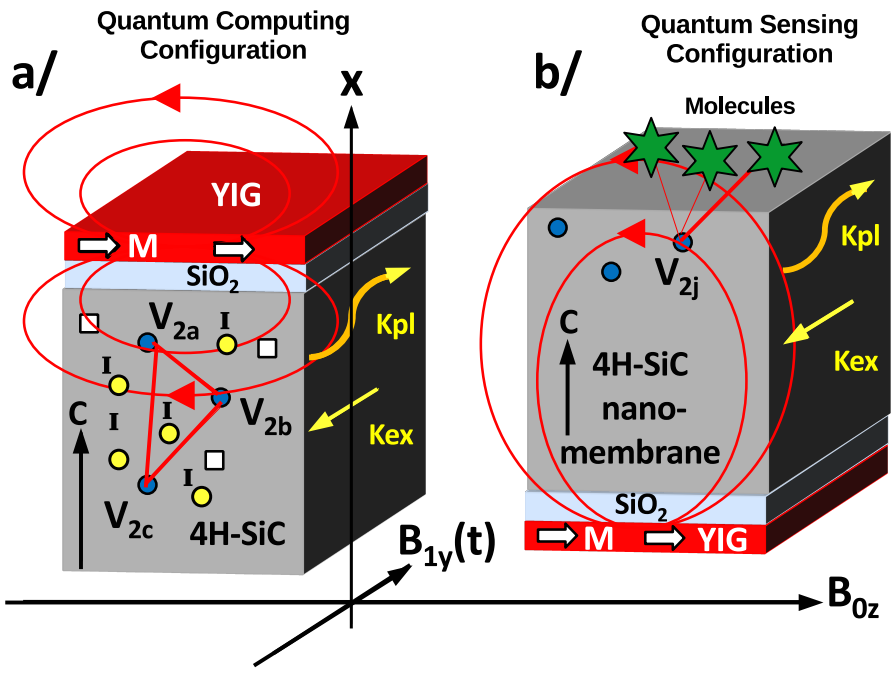

Figure 1: Drawings showing silicon vacancies spin qubits (blue dots) in SiC in dipolar interaction with the stray field of a YIG nanostructure (in red), and a/, also in dipolar couplings between themselves (blue dots) and eventually also with nuclear spins $I=\frac{1}{2}$ (yellow dots), like ^{29}Si or ^{13}C, or other electron spins (white squarres), for Quantum Information processing/storage/communication (note that here V2 qubits are few hundreds of nm below SiC surface), and b/, also in dipolar couplings with external paramagnetic molecules (green stars) for external spins Quantum Sensing (note that here V2 qubits are few nm below SiC surface). V2a, V2b, V2c and V2j are assumed to be shallow V2 type silicon vacancies spins qubits in 4H-SiC, with the c axis along x. Boz is the static external magnetic field applied, B1y(t) is the microwave magnetic field applied, with a frequency around 9.5 GHz (X band). ODMR of shallow V2 spins in those quantum devices require excitation of the photoluminescence (exciting laser light with wave vector kex), and detection of the photoluminescence (photoluminescence with wave vector kpl). See also cited references.[4,7,8]

vacancies defects created by this implantation. This was for example demonstrated for the creation of arrays of silicon vacancies color centers at <z>= 42 nm, with a longitudinal straggling of 35 nm, using 30 keV C^+ ions implantation in SiC.[11] While this might be an interesting approach for fabricating a SiC quantum processor using Vsi silicon vacancies spin qubits, this is still a too large distance from the surface for quantum sensing based on spin-spin dipolar couplings. A more recent study investigated the possibility to bring silicon vacancies spin qubits exactly at the surface of SiC using ion implantation in SiC followed by controlled reactive ion etching of SiC.[13] This study confirmed the feasability of creating very shallow silicon vacancies near the surface, but no

information about their intrinsic quantum spin coherence properties, depurated from inhomogeneous effects and ensemble effects, could be obtained, such that we cannot conclude whether this approach is detrimental or not to their usefull intrinsic quantum spin coherence properties.

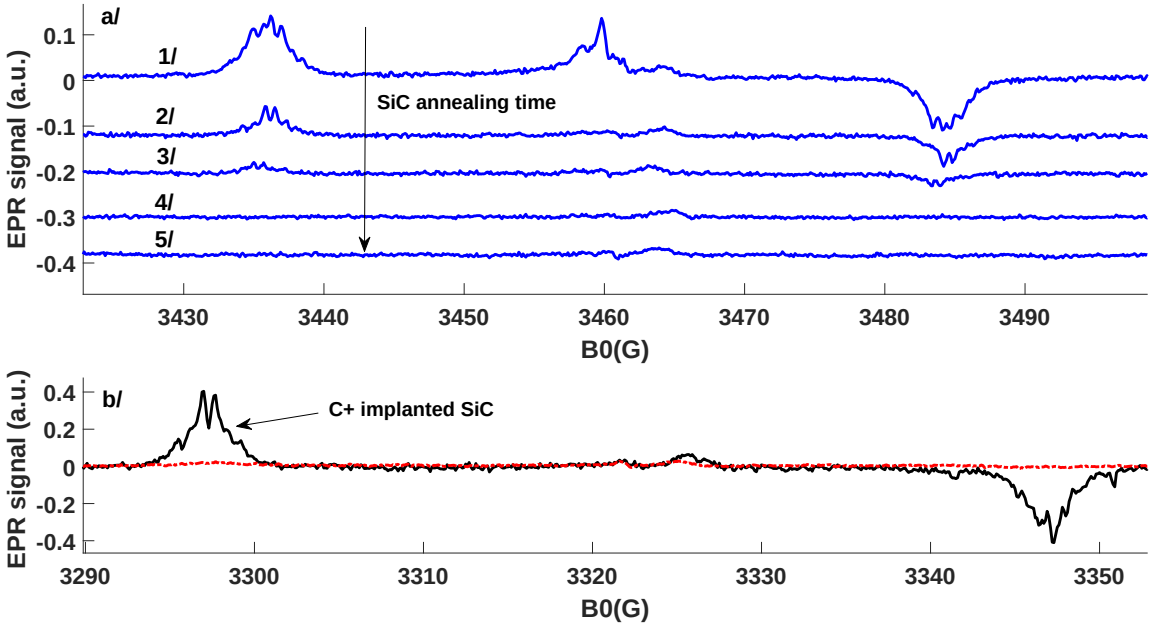

Figure 2: a/ Optical Pumping assisted CW EPR study at RT of the effect of annealing time at 1100 degree C under Argon, on V2 spins in bulk 4H SiC and on other intrinsic defects: 1/ as received bulk 4H-SiC not annealed, 2/ 30 minutes annealed, 3/ 14 h annealed, 4/ 4 days annealed, 5/ 8 days annealed. Laser at 785 nm, P=32 mW; B0 parallel to c axis of 4H-SiC, MD5 cavity, microwave frequency f=9.7 GHz. b/ again CW EPR under OP: comparison between 8 days annealed 4H-SiC sample and the full processesed 4H-SiC sample ion implanted (see text); Laser at 785 nm, P=44 mW; RT, B0 parallel to c axis of 4H-SiC, MS3 cavity, f=9.3 GHz.

Here we investigated a new methodology for creating very shallow Vsi spin qubits in SiC and we performed a detailed investigation of their intrinsic spin quantum coherence properties. The new fabrication method (see Suppl. Info. for details) starts by a high temperature annealing of the HPSI 4H-SiC substrate at $1100\,^{\circ}C$ to remove growth induced silicon vacancies (see Fig.2a), and then basically consist in implanting low energy C^+ ions in SiC but through a thin sacrificial thermal oxide layer of SiO_2, the energy of the C^+ ions being chosen, with the help of SRIM simulation (see Suppl. Info.), such that the maximum of silicon vacancies produced occurs near

the SiO_2/SiC interface. As a result, after a simple full HF chemical etching of the oxide layer, we obtain a nearly half gaussian distribution of silicon vacancies below the SiC surface, whose creation can be revealed by CW photo-EPR (see Fig.2b) and photoluminescence (see Suppl. Info.). We then started our magnetic resonance study by demonstrating fiber based ODMR detection of this ensemble of shallow V2 color centers spin qubits at X band, as it is shown on Fig.3a. This X band ODMR spectrum observed at T=130K under optical pumping and when the magnetic field was applied parallel to the C axis of 4H-SiC, revealed a 50 G splitting between the two lateral EPR transitions associated to the spin $S = \frac{3}{2}$ of the V2 silicon vacancies in 4H-SiC.

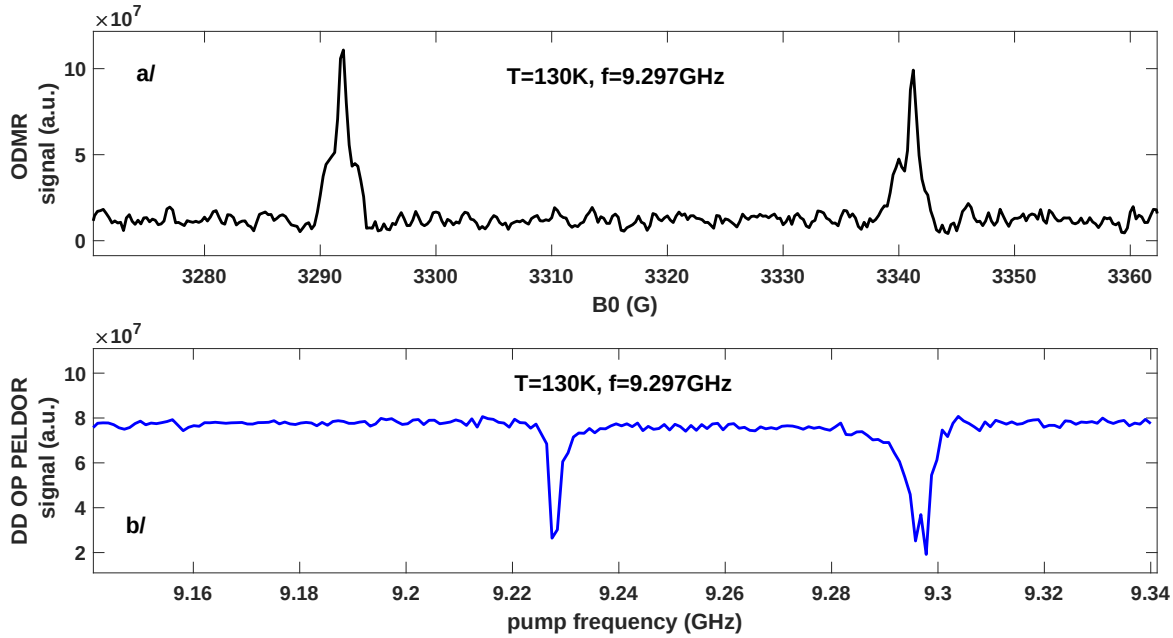

Figure 3: a/ ODMR spectrum of shallow V2 spins of the fully processed ion implanted 4H-SiC sample at T=130K, X band, Plaser= 40 mW at 785 nm, Pi pulse train and continuous optical pumping used; b/ OP-DD-PELDOR spectrum of shallow V2 spins of the fully processed ion implanted 4H-SiC sample at 130K, Plaser= 40 mW at 785 nm.

This is in good agreement with their well know spin hamiltonian:[1,2,4] $H = g\mu_B \vec{B_0}.\vec{S} + D\left(\vec{S}.\vec{e_c}\right)^2$, with $\vec{e_c}$ the unit vector along the C axis of 4H-SiC, $g = 2.0028$ and $D = 35\,MHz$, this 50 G splitting corresponding to $\frac{4D}{g\mu_B}$, as expected. Note that the central EPR transition (+1/2 <–> -1/2) is not observed under optical pumping, because optical pumping at 785 nm equalizes the populations of this two spin levels.

We then performed optical pumping assisted direct detected pulsed electron-electron double resonance experiments at X band (OP-DD-PELDOR) to search for some electron spin bath in interaction with our shallow V2 spin qubits. This OP-DD-PELDOR spectrum, obtained following our previsously demonstrated methodology,[4] is shown on Fig.3b. Two minima or dip in the spin echo amplitude are observed on the spectrum of Fig.3b. The main dip at around 9.296 GHZ corresponds to the shallow V2 spins used as spin probes for external spins quantum sensing (V2 EPR transition (+3/2 <–> +1/2) also observed at 3291.6 G on Fig.3a). The smaller dip at around 9.227 GHZ corresponds to external spins located in the near local environment of the shallow V2 spin probes. It is well known that in 4H-SiC many paramagnetic centers, including carbon related defetcs, exhibit a central EPR line corresponding to a g factor equal or close to $g = 2.0028$, corresponding here, to the dip at around 9.227 GHz for an applied field fixed at 3291.6 G. The OP-DD-PELDOR spectrum of Fig.3b thus demonstrates that the microwave drive at the microwave pump frequency of this electronic spin bath at 9.227 GHz reduces the spin coherence and thus the spin echo amplitude of the nearby shallow V2 spin probes observed at the probe microwave frequency of 9.296 GHz. The precise nature of this electronic spin bath is not clear, but what is clear is that this driven decoherence can be easily suppressed if one avoids to pump with microwave this spin bath. However, this electronic spin bath can also have a passive detrimental effect on the spin coherence of the nearby V2 spins to which it is dipolar coupled, through their thermal fluctuations. However, as we will show it in the next section, it is possible, to some extent, to freeze this spin bath at low temperature such that their impact on the decoherence of the nearby shallow V2 spins could be reduced. To investigate the passive action of this electron spin bath present nearby the shallow V2 spins, we thus performed Hahn spin echo decay experiments at several temperatures, searching for a spin bath cooling effect visible on the V2 spin coherence time T_2 extracted from such an experiment.

The Fig.4 shows three Hahn spin echo decay curves measured at 297K (RT), 130K and 28K respectivelly, as well as their fit by a stretched exponential, with a characteristic decay time $T_{2,Hahn}$ and a stretching exponant n_{Hahn}. Such a stretched exponential decay was already observed in

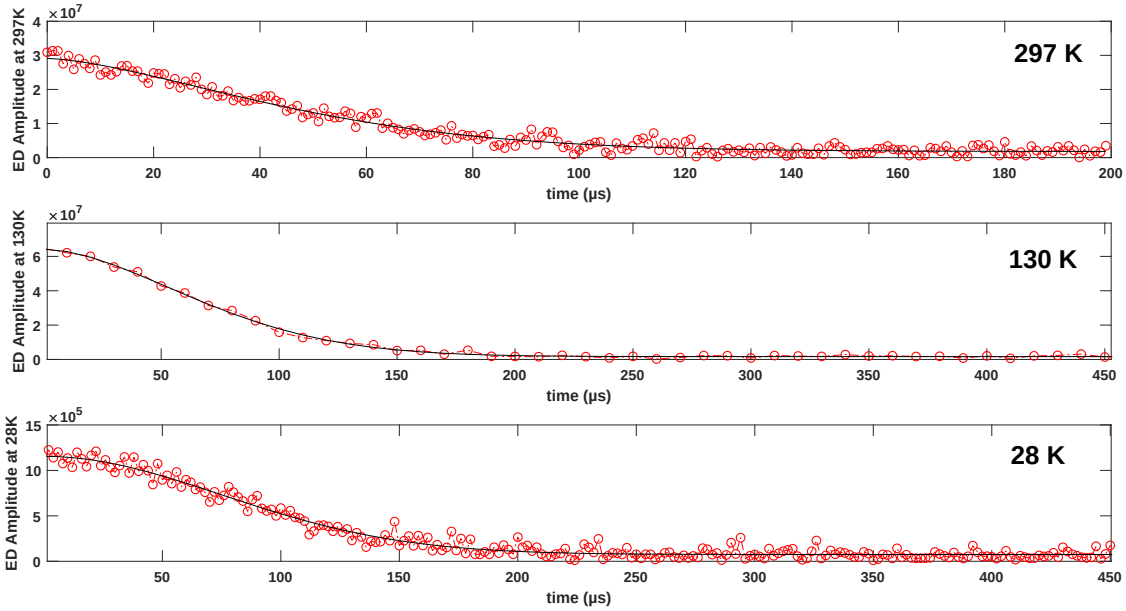

Figure 4: Three Hahn echo decay curves of the shallow V2 spins of the fully processed ion implanted 4H-SiC sample recorded at various temperature and at X band (f=9.3 GHz), with B0 parallel to c axis of 4h-SiC, with Plaser= 45 mW at 785 nm, echo recorded on the low field EPR line of V2 spins, using two steps phase cycling; from top to bottom: T= 297 K, 130 K, 28 K.

the case of NV centers in diamond in interaction with a nearby electronic spin bath.[17] Theory also predicts a stretched exponential decay of the Hahn spin echo due to such kind of electronic spin bath,[17] with a stretch exposant equal to $n_{Hahn} = 1$, for a rapidly fluctuating electron spin bath, thus at high temperature, which should evolve towards $n_{Hahn} = 3$, for a slowly fluctuating electron spin bath, thus at low temperature. We found experimentally that the stretching exponant evolved according to $n_{Hahn}\,(297\,K) = 1.54$, $n_{Hahn}\,(130\,K) = 1.77$, $n_{Hahn}\,(28\,K) = 1.98$, and that in the same time, $T_{2,\,Hahn}$ evolved according to $T_{2,\,Hahn}\,(297\,K) = 55\,\mu\,s$, $T_{2,\,Hahn}\,(130\,K) = 84\,\mu\,s$, $T_{2,\,Hahn}\,(28\,K) = 107\,\mu\,s$. This behavior is thus in good agreement with the theoretically expected one[17] describing passive decoherence of the shallow V2 spins induced by thermal fluctuations of the nearby electronic spin bath. This also confirms the possibility to reduce somehow this passive spin bath decoherence effect simply by thermal cooling.

To further eliminate possible spin-lattice relaxation effects from this previous analysis of the Hahn echo decay, we checked that T_1 (in fact both $T_{1,\,bright}$ and $T_{1,\,dark}\,(130\,K) = 4.8\,ms$, depending

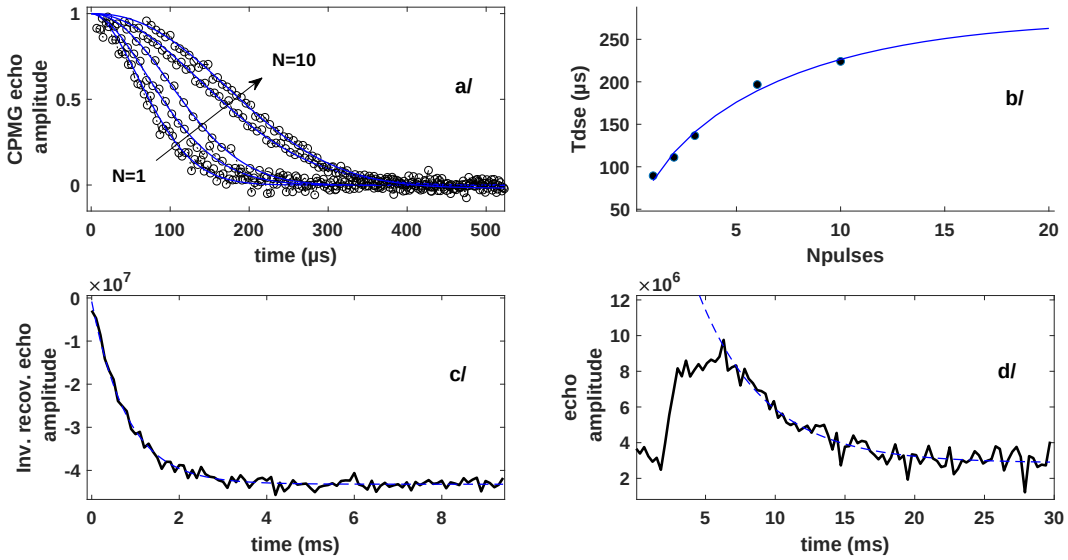

Figure 5: a/ CPMG dynamical decoupling echo decay curves at T= 100 K of the shallow V2 spins of the fully processed ion implanted 4H-SiC sample recorded for Npulses= 1,2,3,6,10, at X band (f=9.3 GHz), with B0 set at an angle of 20 degree with respect to the c axis of 4H-SiC, which is the normal of the sample; Plaser= 43 mW at 785 nm; 7 μs delay between successive Pi pulse used in the CPMG sequence; echo recorded on the low field EPR line of V2 spins, using two steps phase cycling; b/ Spin coherence time under CPMG DD, $T_{2,cpmg}$, as extracted from a stretched exponential fit of the CPMG echo decay curves shown on a/, and presented as a function of the number of Pi pulses in the CPMG DD sequence. $T_{2,cpmg}$ is noted here T_{dse} because it is due to spectral diffusion induced by an electronic spin bath near the V2 spins. c/ and d/ Spin lattice relaxation time, respectively noted $T_{1,bright}$ and $T_{1,dark}$, depending whether continuous optical pumping was used or pulsed optical pumping; we found c/ $T_{1,bright}\,(130\,K) = 814\,\mu s$ and d/ $T_{1,dark}\,(130\,K) = 4.8\,ms$, with Plaser = 40 mW at 785 nm, echo recorded on the low field EPR line of V2 spins at B0= 3291.6 G, f=9.297 MHz.

whether continuous optical pumping was used or pulsed optical pumping), for example at around 130K, was much longer than the $T_{2,Hahn}\,(130\,K) = 84\,\mu s$, as shown on Fig.5c and 5d. This confirmed that spin lattice relaxation do not participate to the main decoherence process which affects the shallow V2 spins, as expected from the known[2] very long spin lattice relaxation times $T_{1,dark}$, which were previously measured for bulk V2 spins.

While cooling the V2 spins and their nearby electron spin bath allows to slightly improve their spin coherence time, it is well known[10] that dynamical decoupling pulsed EPR methods can allow a large increase of the spin coherence time of spin qubits by filtering a large part of the magnetic

noise from their environment to which they are submitted, even at a rather high temperature. Thus, we performed a dynamical decoupling study at $T = 100\,K$ of the effect of Carr-Purcell-Meiboom-Gill (CPMG) type[10] microwave pulse sequences applied to those shallow V2 spins on their spin coherence time, $T_{2,\,cpmg}$ (Fig.5a and 5b). As shown on Fig.5a, under application of CPMG dynamical decoupling pulse sequence involving N_{pulses} Pi pulses, with $N_{pulses} = 1\,,\,2\,,\,3\,,\,6\,,\,10$, we clearly observed an increase of the $T_{2,\,cpmg}$ spin coherence time of the shallow V2 spins and a rapid saturation of $T_{2,\,cpmg}$ with the number of Pi pulses used in the CPMG DD sequence. The detailed analysis of those CPMG DD results (see Suppl. Info.), interpreted in the light of previous results obtained on shallow NV centers,[10] suggests that at 100K, our CPMG filter removes a large part of the low frequency noise due to an electron spin bath sensed by the shallow V2 spins, localized near or at the SiC surface. The saturation value of $T_{2,\,cpmg}$ to $258\,\mu\,s$, extracted from this analysis, reveals another decoherence source not removed by our CPMG filter. We suggest that it is either a high frequency noise (related to some surface phonon in SiC) or an instantaneous diffusion decoherence process[18] related to the local concentration of shallow V2 created near the SiC surface. Further CPMG DD studies, performed with various CPMG filters and various SiC samples implanted at various doses are necessary to determine the precise origine of this $T_{2,\,cpmg}$ limit.

Finally, as we are interested to build hybrid paramagnetic-ferromagnetic SiC based quantum devices,[4,7,8] particularly hybrid SiC-YiG quantum devices,[4,7] here we present our first experiments in this direction, demonstrating the magnetic interaction between V2 spins in SiC and a nearby ferrimagnetic thin YIG film. In practice we used our 4H-SiC sample with shallow V2 spins and we used a commercial thin film of YIG (insulating ferrimagnetic oxide: $Y_3Fe_5O_{12}$, film thickness: 210 nm, normal direction to sample plane: <111>) of high quality, grown by liquid phase epitaxy (LPE) on a GGG substrate. We first checked by Ferromagnetic Resonance (FMR) Experiments performed at X band and RT versus the angle of the applied magnetic field with respect to the <111> axis of YIG, that the FMR rotational pattern was well simulated assuming Bsat=1700 G for the YIG thin film (Fig.6). Then, we put the two samples in close contact and then looked for a signature of their dipolar magnetic interaction through the dipolar stray field produced by the YIG

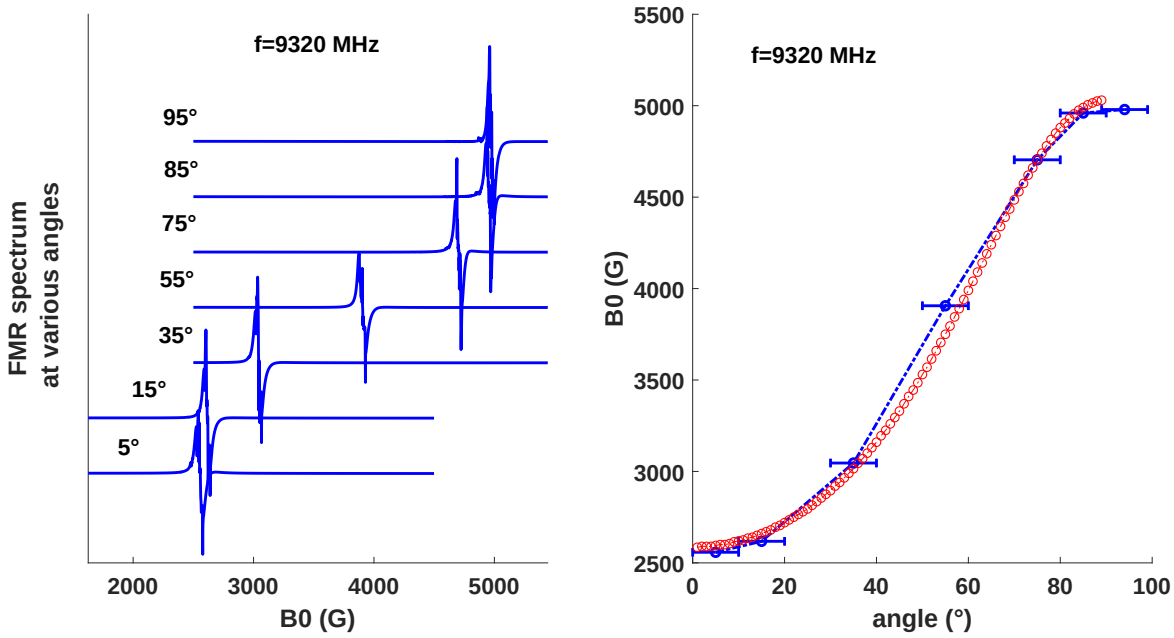

Figure 6: left/ Several Ferromagnetic resonance spectrum (FMR), obtained at X band and RT and at various magnetic field orientation, of a YIG thin film on GGG substrate, which was used in this study. The angle indicated is the one between the applied magnetic field and the <111> direction of YIG, which is also the normal of the sample. An angle of 90 degree corresponds here to the case when B0 and the normal of the YIG film are parallel. right/ Extracted FMR rotational pattern (magnetic resonance field versus angle, dashed dot blue line), as well as its numerical simulation (red dot line) without any free parameter (Bsat= 1700 G and g=2.00 fixed).

thin film on the nearby V2 spins. The Fig.7 shows two V2 spin echo field sweep spectrum recorded in this experimental situation but with two different orientations of the static magnetic field applied with respect to the normal of the two solid samples in contact, as shown on the drawings of Fig.7. Note that the normal of the two samples corresponds both to the c axis for 4H-SiC and to <111> for YIG. The detailed analysis of those two V2 spin echo field sweep spectrum (see Suppl. Info.) shows that in the two orthogonal configuration tested, the paramagnetic resonance lines of the V2 spins are shifted, and that those shift are of opposite sign.

The quantitative analysis of those shift of few Gauss (See Suppl. Info.), by means of standard magnetostatic calculations, suggests that magnetic disks in this 210 nm thick YIG film, having an average diameter close to 60 μm, can well reproduce the dipolar stray magnetic field sensed by the V2 spins in SiC, which is responsible of their magnetic resonance shift. An open question

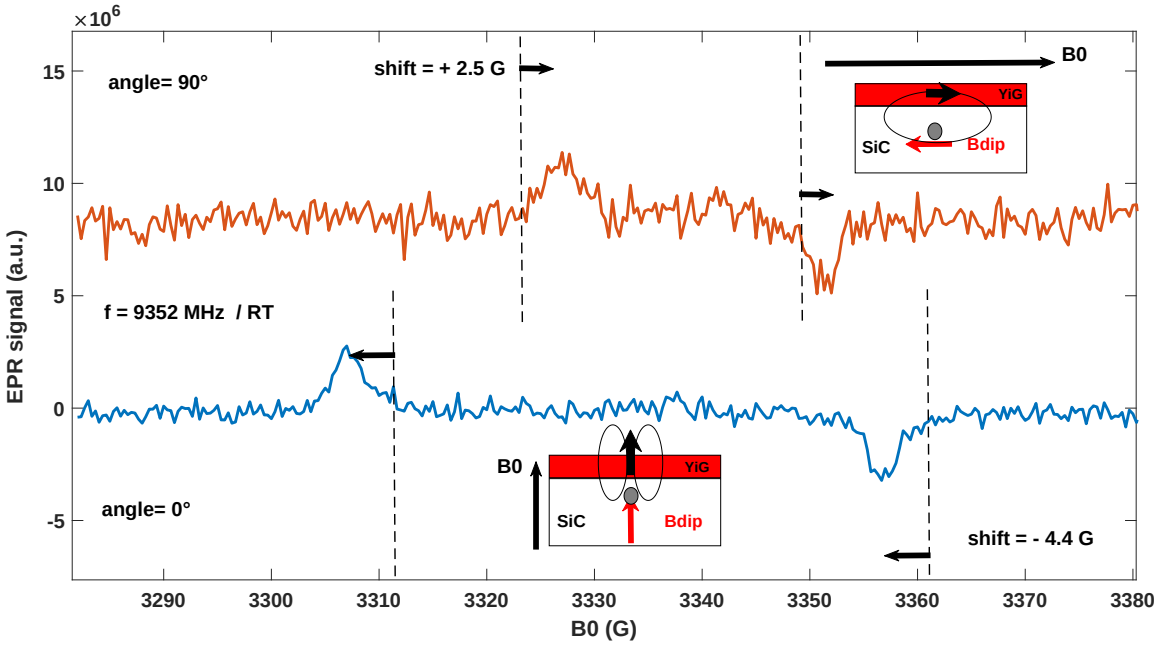

Figure 7: Two V2 spin echo field sweep spectrum recorded at RT, with f=9352 MHz, on the fully processed ion implanted 4H-SiC sample put into contact with a 210 nm thick YIG film on GGG substrate. Two different orientation of the static magnetic field applied with respect to the normal of the two solid samples in contact are presented. The normal of the two samples corresponds both to the c axis for 4H-SiC and to <111> for YIG. Top/ The field direction applied was perpendicular to the normal of the two solid samples and Bottom/ the applied field was parallel to the normal of the two solid samples. The two spectrum reveal shifts of few Gauss of the expected V2 magnetic resonance positions, which are found in opposite sens for those two configuration.

remains however, which is the interpretation of such magnetic disks of $60\,\mu m$ in diameter in a YIG film considered in the fully saturated regime of its magnetization, where no static magnetic domains are expected. We suggest here that the magnetic dipolar couplings between V2 spins and nearby YIG spins combined with the intense resonant microwave drive of V2 spins used in those experiments, can produce some drive of one or few ferrimagnetic spin wave resonance mode of the YIG film. In this picture, the ferrimagnetic magnon coherence length would probably be involved in this experiment. We note that previous studies of spin wave propagation in YIG have shown that the YIG magnon coherence length can reach $31\,\mu m$ in YIG (100 nm)/Pt waveguide structures,[20] despite the enhanced damping due to metal Pt. As here we use a YIG film (210 nm) on GGG substrate, with an expected lower spin wave damping, it seems reasonable to assume

a ferrimagnetic magnon coherence length in our sample on the order of $60\,\mu\,m$. The detailed investigation of this question is beyond the scope of this paper. What is clear however, is that the observed shifts of opposite signs in the two configurations tested can not be explained by the standard spin hamiltonian of V2 spins ($H = g\,\mu_B\,\vec{B_0}.\vec{S} + D\left(\vec{S}.\vec{e_c}\right)^2$) and are thus due to the presence of the nearby YIG film, introducing an additional dipolar coupling hamiltonian between V2 spins and nearby YIG spins. Those experiments thus constitute a demonstration of external YIG spins sensing by means of V2 spins in 4H-SiC, through dipolar magnetic couplings.

3 Discussion

Let us now discuss the relevance of the shallow implanted V2 spin qubits we successfully fabricated here in the context of planed quantum sensing and quantum computing applications. In our previous theoretial work on the SiC-YIG OD-PELDOR quantum sensor,[7] capable of sensing at nanoscale the electron spin labels of a nearby large target protein or the spin qubits of a nearby large paramagnetic molecular nanocrystal (Fig.1b), we underlined the need of having a shallow V2 spin probe with a sufficiently long spin coherence time. More precisely, in ODPELDOR, the maximum distance that can be measured between target and probe spins is determined by the maximum dipolar evolution time, such that $20\,\mu\,s$ are necessary to measure a distance of 10 nm, and $60\,\mu\,s$ are necessary for measuring a distance of 15 nm. As the nano-object of interest for SiC-YIG ODPELDOR sensing at nanoscale will have a diameter of 10 nm or more, one immediatly concludes that a shallow V2 spin qubit, located within the first 5 nm below the SiC surface and having a spin coherence time of at least $60\,\mu\,s$ is required. As a long T1 of the dark spins (spin labels or remote qubits) is also necessary,[7] which almost always implies cooling the whole sample at or below 100K, having $T_2\,(T = 100\,K) = 60\,\mu\,s$ for the V2 shallow spin probe is what we need in practice. Here, we have demonstrated that our shallow silicon vacancies V2 spin qubits are dipolar coupled to an electronic spin bath, which seems localized near the SiC surface considering our first OPPELDOR and CPMG Dynamical Decoupling (DD) experiments. This spin bath limits the shallow

V2 spin coherence time to around $T_2 = 84\,\mu s$ at 130K, without DD, which is however sufficient to perform the planned nanoscale resolution OD-PELDOR experiments applied to structural biology. We also showed that T_2 can reach around $100\,\mu s$ at 28K without DD, which offers some further improvement. Extending T_2 up to $220\,\mu s$ at 100K by CPMG DD has also been demonstrated here, also suggesting that further improvements by DD are possible, even at 100K. It must be also noted that surface passivation or surface capping has not been tested here, and this could also allow futur improvements by eliminating or diluting the surface electronic spin bath which limits T_2 without CPMG DD. It must be also underlined that here we performed spin ensemble measurements, such that $T_2 = 84\,\mu s$ at 130K has to be considered as an average value, and future single shallow V2 spin experiments may reveal some distribution of T_2 values depending on the local surface spin bath concentration experienced by those shallow single V2.

Finally, let us discuss our results in the context of quantum computing with V2 spin qubits introduced by ion implantation in a SiC quantum device. Even simply considering single qubit quantum gates, generally performed using short resonant microwave pulses (a typical Pi pulse in a 3D microwave cavity last 30 ns), one would need at least $T_2 \geq 300\,\mu s$ to go beyong the $\frac{T_2}{T_{gate\,1\,Q}} \geq 10^4$ threshold previously established for fault tolerant quantum computing.[19] $T_2 = 100\,\mu s$ at 28K without DD is thus not sufficient for fault tolerant quantum computing with this kind of shallow V2 spins. Extending T_2 up to $220\,\mu s$ at 100K by CPMG DD has been demonstrated here for our shallow V2 spin qubits, but it is still limited by either surface phonon or by the instantaneous diffusion related to the too high local concentration of such shallow V2 spin qubits created by ion implantation. However, assuming one wishes to perform quantum simulations on a diluted cluster of dipolar coupled V2 spins (or a mixture of V2 and V1 silicon vacancies spin qubits), created by ion implantation at low dose and submitted to the strong dipolar magnetic field gradient produced by a nearby YIG nanostripe, located at an optimal distance of $x_{opt} = 150\,nm$ from V2 spin qubits[7,8](see Fig.1), then in that case, we see we do not need anymore the very shallow V2 spin qubits used for OD-PELDOR quantum sensing. One just needs here V2 spins located between 100 nm and 200 nm below the SiC surface for quantum computing. In that case, the V2 spins should become

strongly isolated from the intrinsic surface noise of SiC, which is detrimental to their T_2, and also from the noise related to thermal fluctuations of the nearby ferrimagnetic YiG nanostripe.[7,8] If one assumes that at such a large distance from the surface of SiC, the V2 spins have spin coherence properties similar to those previously measured for bulk V2 spins,[2] then one expect to extend the T_2 of such nearly bulk V2 spin qubits up to $T_{2,cpmg} = 45\,ms$ at 17K using a 10^5 CPMG DD pulse sequence, as it was previously demonstrated at lower magnetic field.[2] It was also deduced by extrapolation that using a 10^7 CPMG DD pulse sequence, one could reach $T_{2,cpmg} = 300\,ms$ at 17K.[2] Now, considering two V2 electron spins in the V2 cluster separated by a distance of 10 nm, one would need typically a dipolar evolution time of around $20\,\mu s$, as already discussed above in the ODPELDOR quantum sensing context, to perform a two qubit quantum gate, such that one would need $T_2 \geq 200\,ms$ to go beyong the $\frac{T_2}{T_{gate2Q}} \geq 10^4$ threshold requiered for fault tolerant quantum computing with such a diluted cluster of V2 spins. Thus, using a ion implanted cluster of nearly bulk V2 spins located few hundreds of nanometers below the SiC surface, using intensive dynamical decoupling microwave pulse sequences below 17 K, using the strong magnetic field gradient produced by a nearby YiG ferrimagnetic nanostripe (between 0.1 G/nm and 0.5 G/nm),[7,8] and using resonant selective optical and microwave manipulations[6] of the various V2 spin qubits, it seems feasible to perform fault tolerant quantum computing at X band (10 GHz) using an hybrid SiC-YIG quantum device, such as the one shown on Fig.1a. Adding one or few V1 silicon vacancies (or few other SiC color centers more appropriate for quantum communication) to this V2 cluster of spin qubits would also offer interesting possibilities for an optical fiber based spin-photon interface[5] compatible with the proposed experimental approach,[7] and which could be usefull for extending the scalability of such an intermediate-scale fault-tolerant hybrid SiC-YIG quantum computing approach.[7,8] As a last remark, we note that diluted non-zero nuclear spins in the SiC device, like those of ^{29}Si or ^{13}C, present from growth or introduced by ion implantation nearby the cluster of V2 spin qubits, could also be used as a quantum ressource,[5] both for long term storage of quantum states, and for extending the scalability of such an intermediate-scale fault-tolerant hybrid SiC-YIG quantum computer without using the spin-photon interface.

4 Conclusion

In conclusion, here we have demonstrated i/ a new methodology for creating shallow VSi spin qubits located at nanoscale distance below the SiC surface by low energy ion implantation through a sacrificial SiO_2 layer, ii/ that those shallow Vsi spin qubits are dipolar coupled to an electronic spin bath, probably localized near or at the surface, analysing Hahn echo decay, dynamical decoupling (DD), and OP-PELDOR experiments, iii/ that their coherence time increase with cooling the spin bath (from 55μs at 297K, to 84μs at 130K, and to 107μs at 28K), and that it can be further extended to 220μs at 100K by DD. At temperatures below 130K, with or without DD, the spin coherence time of those shallow V2 spin probes is thus clearly sufficient for OD-PELDOR quantum sensing applications. Finally, iv/ we demonstrated the shift of the shallow V2 spin qubits magnetic resonance induced by the stray field of a nearby YIG film. This demonstrates external YIG spins sensing by V2 spins in SiC. This work thus constitutes a promising step towards the development of the recently proposed SiC-YIG hybrid quantum devices, for both nanoscale ODPELDOR quantum sensing and for spin based fault tolerant quantum computing technologies, which have both the advantage that they could be fiber integrated to a state of art commercially available pulsed EPR spectrometer, offering a wide access to those intermediate scale quantum technologies.

5 Supplementary Information

Details on the fabrication of shallow silicon vacancies.

First, we start with a high purity and semi-insulating commercial 4H-SiC wafer. Due to growth, this substrate already contains many bulk defects, including the silicon vacancies defects we are interested in here. As it is well known that those silicon vacancies spin qubits color centers can be removed by a high temperature annealing typically above $800\,^{\circ}C$, we started by a long $1100\,^{\circ}C$ thermal annealing under argon gaz of this wafer. As it is shown on Fig.2a, a cw EPR (electron paramagnetic resonance) study of this annealing process, called the Reset process, was performed at room temperature under optical pumping. It is clearly seen on Fig.2a that after 8 days of such an

annealing, the photo-EPR signal of V2 type silicon vacancies at X band (around 9.7 GHz) was no more detected. Using other reference pieces of this wafer, and using profilometry and ellipsometry experiments (not shown), we determined the oxidation rate of 4H-SiC by thermal oxidation under pure Oxygen at $1100\,^{\circ}C$, as well as the chemical etching rate of the resulting SiO_2 layer by a diluted solution of HF. In our experimental conditions, we found an etching rate close to 63 nm per minute, thus of roughly 1 nm per second. Of course, slower or faster etching rates of SiO_2 on SiC could be designed, depending on the HF solution concentration. Controlling the 4H-SiC oxidation rate and the SiO2 chemical etching rate, we fabricated a 74 nm oxide layer on our Reset and oxidized 4H-SiC wafer, which was then used as a sacrificial layer for the subsequent ion implantation process. SRIM simulation indicated that for such a system, SiO_2 (74 nm)/4H-SiC(infinite), C^+ ions having an energy of around 23 keV would produce a maximum of silicon vacancies near the SiO_2/4H-SiC interface. Thus, 23 keV C^+ ions were implanted through this 74 nm oxide layer at a dose of $2\,10^{13}\,cm^{-2}$. The SiO2 was then removed from the implanted 4H-SiC sample by a full HF etching, producing a nearly half gaussian distribution of silicon vacancies below the SiC surface, with a maximum at the surface and a half width of around 25 nm, according to SRIM simulations (see further). Finally, as we wanted to activate a large enough ensemble of those shallow silicon vacancies created by ion implantation, we then performed a post implantation annealing of 90 minutes at $700\,^{\circ}C$ under argon gas, in order to optimize the amount of shallow silicon vacancies of V2 type in this implanted 4H-SiC sample. Still using CW photo-EPR, we clearly observed the re-appearance of the silicon vacancies in our 4H-SiC sample as a result of this ion implantation process (see Fig.2b), as requiered for a full pulsed EPR study of their quantum spin coherence properties.

Fig.8 shows the result of a SRIM numerical simulation of the ion implantation process in 4H-SiC through a sacrificial SiO2 layer, used here to create shallow V2 spins.

The Fig.9 compares the V2 infrared photoluminescence spectrum of the 8 days annealed 4H-

SiC reference sample and the one of the fully processed and ion implanted 4H-SiC sample studied here in details.

All the magnetic resonance experiments presented here were performed on a commercial ELEXYS E580 pulsed EPR spectrometer from BRUKER operating at X band (9.3 - 9.7 GHz). This pulsed EPR spectrometer was interfaced by means of an optical fiber to a standard external photolminescence setup, allowing both laser light excitation at 785 nm and photoluminescence collection and detection, following previously published methodologies for fiber based OP-pulsed EPR, OP-PELDOR and ODMR.[4,7]

Details on the analysis of CPMG DD experiments on the shallow V2 spins.

Following the previously described method used for shallow NV centers in diamond,[10] we extracted $T_{2,cpmg}$ from a stretched exponential fit ($exp\left[-\left(\frac{t}{T_{2,cpmg}}\right)^{\alpha}\right]$) of the echo decay under CPMG sequence. As shown on Fig.5a, under application of CPMG dynamical decoupling pulse sequence involving N_{pulses} Pi pulses, with $N_{pulses} = 1, 2, 3, 6, 10$, we clearly observed an increase of the $T_{2,cpmg}$ spin coherence time of the shallow V2 spins (respectively, $T_{2,cpmg}$ in μs and α were found to be: (89,1.86), (111,1.79), (136,2.06), (197,1.99), (224,2.28)). To further investigate the nature of the noise filtering effect of this CPMG pulse sequence on the electronic spin bath nearby the shallow V2 spins, we plotted on Fig.5b, $T_{2,cpmg}$ as a function of N_{pulses}, the number of Pi pulses in the CPMG sequence. We observed a saturation effect with respect to N_{pulses}, starting at a low value of N_{pulses}. This effect was previously observed for isolated shallow NV centers in diamond.[10] In this previous study on isolated shallow NV centers, the data were fitted by a function of the type $T_{2,cpmg}\left(N_{pulses}, N_{sat}, k, T_{2,1p}\right) = T_{2,1p}\left(N_{sat}^{k} + \left(N_{pulses}^{k} - N_{sat}^{k}\right) e^{-\frac{N_{pulses}}{N_{sat}}}\right)$. For shallow NV centers in diamond located 20 nm below the surface, the fit reported gave the parameter $k = 0.53$, close to the $k = 2/3$ expected for a simple lorentzian spin bath,[10] while for very shallow NV centers in diamond (2 or 3 nm below the surface), the fit reported gave the parameter k in the range $[0.30, 0.48]$.[10] Concerning the parameter N_{sat} found for shallow NV centers

in diamond, it was found in the range $[13\,,\,200]$,[10] depending on the depth and surface properties of the diamond surface. Here, the fit of our CPMG results at T=100K on shallow V2 spins in 4H-SiC provided the parameters: $N_{sat} = 17.38$, $k = 0.44 +/- 0.1$, $T_{2,1p} = 73360\,ns$, and thus an optimal shallow V2 spin coherence time in SiC with our CPMG noise filtering sequence of $T_{2,cpmg\infty} = 258\,\mu s$, which can be reached with a good approximation using $N_{pulses} \geq\geq N_{sat} = 17$. The value $k = 0.44 +/- 0.1$ that we found is close to the values observed for isolated shallow NV centers. This is somehow expected here because we performed CPMG experiments on V2 spins ensemble, distributed according to SRIM after C+ ion implantation, mainly between 0 nm and 25 nm below the SiC surface. This value of $k = 0.44 +/- 0.1$ is however closer to the values found for very shallow NV centers in diamond[10] which were more exposed to the surface noise, which was considered as a 2D surface spin bath with a correlation time at room temperature of around $\tau_c\,(RT) = 11\,\mu s$. As here, our V2 spin distribution is expected to be roughly a half gaussian with maximum at the SiC surface, this seems reasonable. This similarity in the k factor value also suggests that in our case the surface noise is also due to an electronic spin bath, as already suggested by our PELDOR experiments (Fig.3b) and Hahn echo decay experiments versus temperature (Fig.4). Note that our CPMG experiments were performed at a fixed delay $\tau = 7\,\mu s$ between the Pi pulses, corresponding to a CPMG filter function centered at around $f_0 = \frac{1}{2\tau} = 71\,kHz$. With $N_{pulses} = 10$, the spectral bandwidth of this CPMG filter is of around $7\,kHz$. Here we found a rapid saturation of $T_{2,cpmg}$ with the number of Pi pulses. This is also somehow expected because by cooling our 4H-SiC sample at T=100K, the spin bath is also cooled and thus its correlation time becomes longer, typically on the order of the spin lattice relaxation time of the spin specy that constitute the surface spin bath at this temperature. Assuming that at 100K, the surface spin bath has a correlation time $\tau_c\,(100\,K) = 1\,ms$ (thus $f_{noise\,cutoff} = \frac{1}{\tau_c} = 1\,kHz$), with an associated spectral density of noise of the form $S(\omega) = \frac{\Delta^2}{\pi}\frac{\tau_c}{1+(\omega\,\tau_c)^2}$ (Δ being the spin qubit - spin bath coupling in this model),[10] then we see that our CPMG filter at $f_0 = \frac{1}{2\tau} = 71\,kHz$ with N=10 removes a large part of this noise. As the CPMG filter becomes narrower and narrower when the number of Pi pulses increase, this could explains why $T_{2,cpmg}$ saturates rapidly with the number of Pi pulses applied in our experimental

conditions.

The remaining question is what is the fundamental decoherence process which remains in our CPMG experiments at T=100K and which is responsible for the ultimate value $T_{2,cpmg\infty} = 258\,\mu s$. Here we suggest two possibilities. Either, like for shallow NV centers in diamond,[10] another noise contribution has to be considered which is related to surface phonon in SiC and which would have a spectral density of noise with a frequency cutoff located at a much higher frequency, like around 10 MHz as it was found for shallow NV centers in diamond.[10] Our CPMG noise filter at $f_0 = \frac{1}{2\tau} = 71\,kHz$ with N=10 could thus not remove efficiently this high frequency noise, which would explain $T_{2,cpmg\infty} = 258\,\mu\,s$. The other possibility, which is possible in our study but which was not possible in the previous study of shallow NV centers, is that $T_{2,cpmg\infty} = 258\,\mu\,s$ is in fact limited by the instantaneous diffusion decoherence process[18] which exist when spin ensemble are studied and which can not be removed by CPMG dynamical decoupling methods. Thus, the ultimate spin coherence time in our sample for the shallow V2 spins would be $T_{2,cpmg\infty} = T_{ID} = 258\,\mu\,s$. To decide between those two possible explanations of $T_{2,cpmg\infty} = 258\,\mu\,s$, one needs to perform a set of similar CPMG noise spectroscopy experiments with various CPMG filter at various filter frequencies, with various bandwidth, eventually at various temperature, and on various samples with various doses of C+ ions implanted below the SiC surface. This is beyond the scope of this study and this is let for a future work.

Detailed analysis of the two shift of opposite sign observed on the V2 magnetic resonance lines when placing a YIG thin film into contact with our implanted SiC sample.

The first field direction applied was perpendicular to the normal of the two solid samples, SiC and YIG (Fig.7 top spectrum), and the second one was parallel to this normal (Fig.7 bottom spectrum). For a magnetic field applied perpendicular to the c axis of 4H-SiC, without YIG and just considering the well known spin hamiltonian $H = g\,\mu_B\,\vec{B_0}.\vec{S} + D\left(\vec{S}.\vec{e_c}\right)^2$, with $\vec{e_c}$ the unit vector along the C axis of 4H-SiC, $g = 2.0028$ and $D = 35\,MHz$, one expects two V2 EPR lines splittted by 25 Gauss, centered around the field resonance value corresponding to $g = 2.0028$ at the fixed mi-

crowave frequency used. For a magnetic field applied parallel to the c axis of 4H-SiC, one expects, without YIG, two V2 EPR lines splittted by 50 Gauss, centered around the field resonance value corresponding to $g = 2.0028$ at the fixed microwave frequency used. We clearly observe on the Fig.7 top spectrum two V2 EPR lines splittted by 25 Gauss as expected in this configuration, but not centered around a field resonance value corresponding to $g = 2.0028$ at the fixed microwave frequency used, but at a higher magnetic field value, corresponding to a shift of around $+2.5\,G$. This shift of the two EPR lines towards higher magnetic field values can be explained if one considers that a dipolar stray magnetic field produced by the YIG magnetic film is sensed by the shallow V2 spins and that it has the same direction as the one of the externally applied magnetic field, but is of opposite sens. This is qualitatively what one expects in this first experimental configuration, as schematically explained by the drawing nearby the Fig.7 top spectrum. We also clearly observe on the Fig.7 bottom spectrum two V2 EPR lines splittted by 50 Gauss as expected in this second configuration, but not centered around a field resonance value corresponding to $g = 2.0028$ at the fixed microwave frequency used, but at a lower magnetic field value, corresponding to a shift of around $-4.4\,G$. This shift of the two EPR lines towards lower magnetic field values can be explained again, if one considers that a dipolar stray magnetic field produced by the YIG magnetic film is sensed by the shallow V2 spins and that it has the same direction as the one of the externally applied magnetic field (along the c axis of SiC, which is also the <111> axis of YIG) and also the same sens. This is qualitatively what one expects in this second experimental configuration, as schematically explained by the drawing nearby the Fig.7 bottom spectrum.

One question remains which concerns the microscopic origin of this dipolar stray magnetic field sensed by the V2 spins in SiC, located below the YIG thin film, which is related to the quantitative analysis of the observed shift in the V2 magnetic resonance position. Indeed, for a uniformly magnetized thin film, with static magnetic domains of infinite dimension, one would expect no dipolar stray magnetic field which could be sensed by the V2 spins in SiC located nearby the YIG film. However, if one makes the hypothesis that we have a typical magnetic length of $60\,\mu m$ involved in this experiment (see text for discussion of its origin), then standard magnetostatic cal-

culations (not shown) allow to explain those two shift of opposite sens, simply assuming magnetic squares (or disk) exist into the YIG thin film, with the dimension of one edge of the square being $a_{edge} = 60\,\mu m$, assuming a film thickness of $210\,nm$, and assuming a saturation magnetization of this YIG film of $B_{sat} = 1700\,G$, as confirmed by our YIG film FMR experiments (Fig.6). More precisely, the calculations show that one expect a dipolar stray magnetic field induced shift of around +2.5 G for the case where V2 spins are located anywhere within the first $6\,\mu m$ below the SiC surface and at the vertical of the center of the magnetic square considered, and when the magnetic field was applied perpendicular to the normal of the two solid samples. Calculations also show that one expects a dipolar stray magnetic field induced shift of -5 G for the case were V2 spins are located anywhere within the first $6\,\mu m$ below the SiC surface and at the vertical of the center of the magnetic square considered, and when the magnetic field was applied parallel to the normal of the two solid samples. The magnetostatic calculations are thus in good quantitative agreement with the experimentally observed shift.

Contributions

JT proposed the study, performed magnetic resonance experiments and analysed them, DM and YLG designed and performed ion implantation of SiC, SR performed the SiC oxydation, SiO2 chemical etching, various SiC processing and profilometry, TF performed various ellipsometry and AFM measurements, JB performed various micro-Photoluminescence measurements. All authors contributed to the manuscript.

Acknowledgments

The authors thanks Yann Le Gall for his contribution to the ion implantation in this study. The authors thanks the University of Strasbourg and CNRS for the reccurent research fundings.

References

(1) M. Widmann et al., Nature Materials **14**, 164 (2015).

(2) D. Simin et al., Phys. Rev. B **95**, 161201(R) (2017).

(3) J.S. Embley et al., Phys. Rev. B **95**, 45206 (2017).

(4) J. Tribollet, Eur. Phys. J. Appl. Phys. 90, 20103 (2020).

(5) R. Nagy et al., Nature Comm. **10**, 1954 (2019)

(6) H.B. Banks, Phys. Rev. Applied 11, 24013 (2019).

(7) J. Tribollet, Eur. Phys. J. Appl. Phys. 90, 20102 (2020).

(8) J. Tribollet et al., Eur. Phys. J. B. **87**, 183 (2014).

(9) S. Castelleto et al., J. Phys. Photonics **2**, 022001 (2020).

(10) Y. Romach et al., Phys. Rev. Letters **114**, 17601 (2015).

(11) J. Wang et al., Phys. Rev. Applied **7**, 64021 (2017).

(12) J. Wang et al., ACS Photonics **4**, 1054 (2017).

(13) Q. Li et al., Nanoscale **11**, 20544 (2019).

(14) S. Agnello et al., Phys. Rev. A **59**, 4087 (1999).

(15) R.N. Shakhmuratov et al., Phys. Rev. Letters **79**, 2963 (1997).

(16) J.F. Ziegler et al., Nuclear Instruments and Methods in Physics Research section B Beam interaction with Materials and Atoms **268**, 1818 (2010).

(17) G. de Lange et al., Science **330**, 60 (2010).

(18) A. Schweiger et al., Principles of pulse electron paramagnetic resonance, Oxford University Press, Oxford UK; New York (2001).

(19) D.P. DiVincenzo, Fortschr. Phys. **48**, 771 (2000).

(20) P. Pirro et al., Appl. Phys. Lett. **104**, 12402 (2014).

Competing financial interests

The authors declare that they have no competing financial interests.

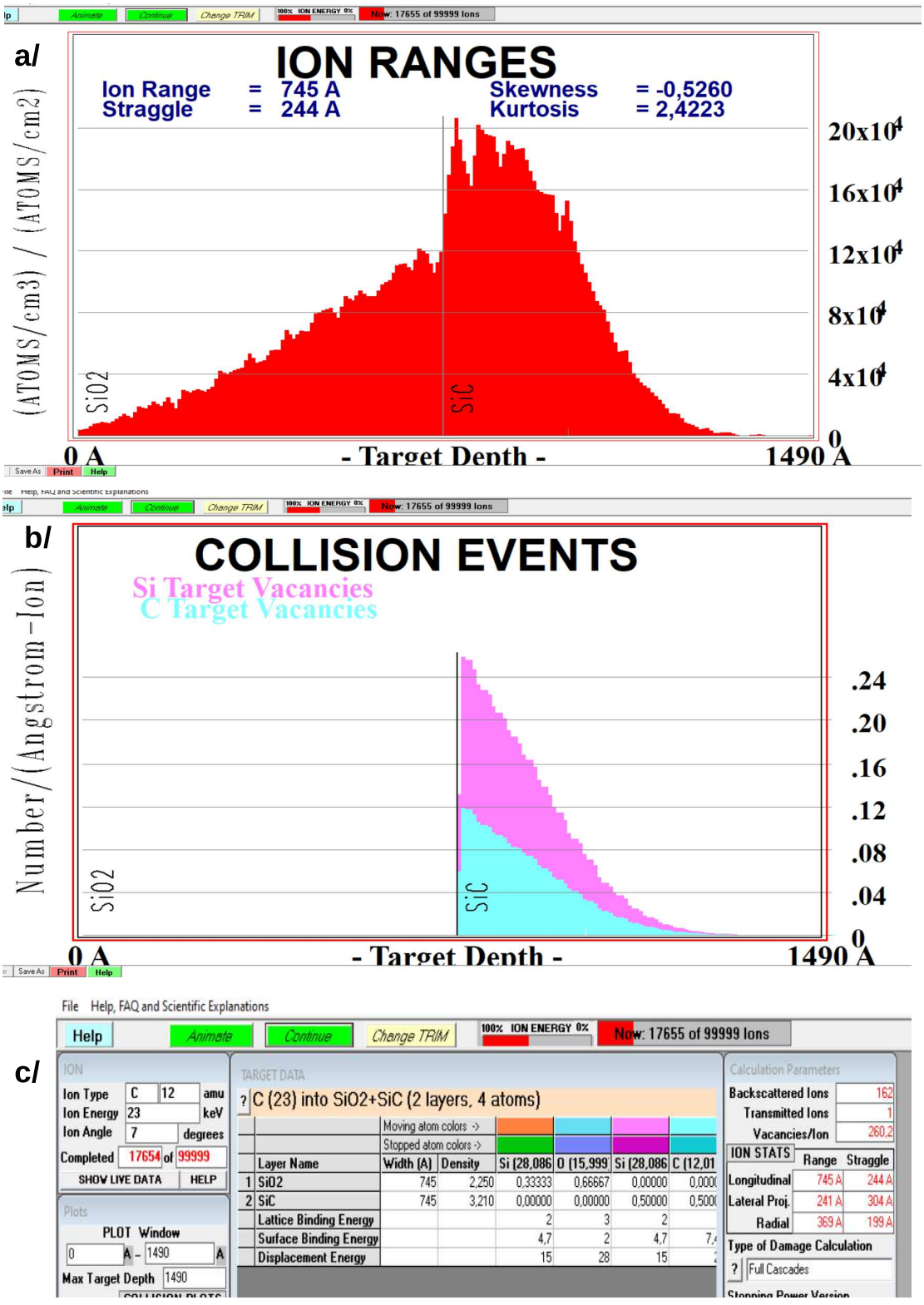

Figure 8: SRIM simulation of the ion implantation process of 23 keV C+ ions through a 74.5 nm SiO2 sacrificial layer present on top of the 4H-SiC substrate pre-processed (see text).

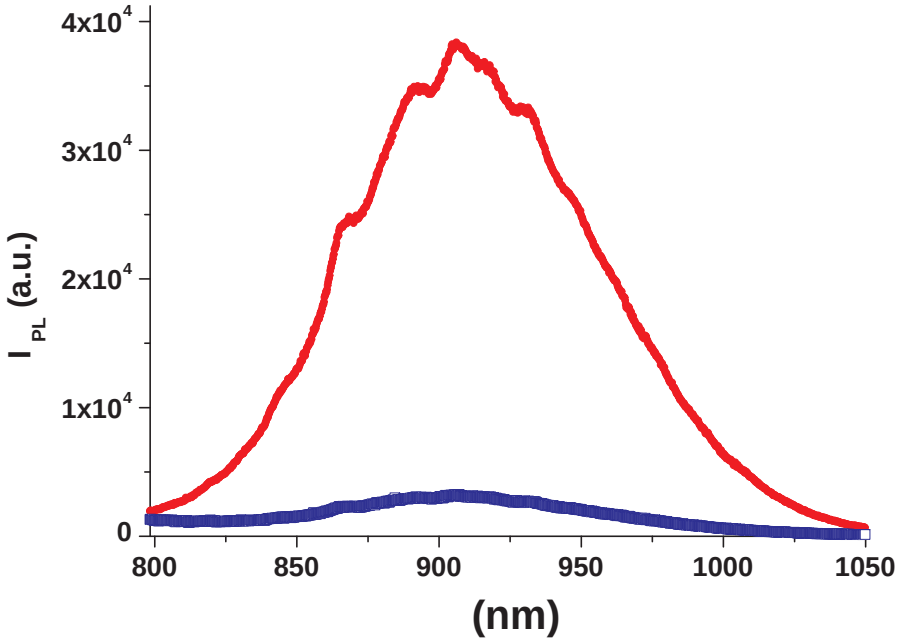

Figure 9: Infrared micro-photoluminescence spectrum of the 8 days annealed 4H-SiC reference sample (in blue) and the one of the fully processed and ion implanted 4H-SiC sample studied here in details (in red). Spectrum obtained on a micro-Raman spectrometer at RT (300K), objective *100, NA=0.9, Plaser= 90mW at 532 nm, Tinteg= 60sec.